Collapse of Telechelic Star Polymers to Water-Melon Structures

Federica Lo Verso, Christos N. Likos, Christian Mayer, and Hartmut Löwen

Institut für Theoretische Physik II,

Heinrich-Heine-Universität Düsseldorf, D-40225 Düsseldorf, Germany

(Dated: February 6, 2008)

Abstract

Conformational properties of star-shaped polymer aggregates that carry attractive end-groups, called *telechelic star polymers*, are investigated by simulation and analytical variational theory. We focus on the case of low telechelic star polymer functionalities, $f \leq 5$, a condition which allows aggregation of all attractive monomers on one site. We establish the functionality- and polymerization-number dependence of the transition temperature from the "star burst" to the "water melon" macroparticle structure. Extensions to telechelic stars featuring partially collapsed configurations are also discussed.

PACS numbers: 61.25.Hq, 82.70.Uv, 36.20.Ey, 61.20.Ja

Self-organizing soft materials are relevant in developing novel macromolecular compounds with peculiar structural and dynamical properties, which are related to mesoscopic aggregation as well as intra- and inter-molecular association [1, 2]. Progresses in the synthesis of chains with attractive end-groups, called *functionalized* or *telechelic polymers*, opened the way for the subsequent synthesis of telechelic star polymers with attractive polar end groups, telechelic associating polymers with hydrophobic terminal groups, associating polyelectrolytes in homogeneous solutions, and telechelic planar brushes [3, 4, 5, 6]. A telechelic star, which is the subject of the work at hand, consists of f chains with one of their ends chemically attached on a common center, whereas the attractive ends are free at the other end of the molecule. Block copolymer stars with a hydrophilic core and a hydrophobic corona [7, 8] also bear similarities to telechelic stars, the two systems becoming identical when the length of the hydrophobic block reduces to a single monomer. The thermodynamics and the structure of planar telechelic brushes have been recently analyzed also from a theoretical point of view, shedding light into the quantitative characteristics of both the conformations and the interactions of the same [9, 10, 11]. Further theoretical approaches have been developed to describe flower-like micelles with hydrophobic terminal groups that self-assemble in water. Such aggregates show a characteristic 'bridging attraction' [9, 12] that can even lead to a liquid-vapor phase transition [13]. The interesting feature of telechelic star polymers is the possibility of attachment between the attractive terminal groups. In dilute solutions, this gives rise to intra-molecular association as well as inter-association between micelles, depending on the details of the molecular structure.

Examples of low-functionality telechelics, very similar to the ones considered in this work, are mono-, di-, and tri-ω-zwitterionic, three-arm star symmetric polybutadienes. Experiments have shown that these self-assemble into distinct supramolecular structures, including collapsed, soft-sphere conformations [4, 14]. In particular, using low-angle laser light scattering and dynamic light scattering, it was found that samples with three zwitterion end groups present a low degree of inter-association between macromolecules, showing instead a preference for intra-association and formation of collapsed soft spheres [3, 15]. X-ray scattering and rheological experiments support the conclusion that this tendency persists at higher concentrations, all the way into the melt [4]. There, the formation of transient gels has been found for the case of two- and three-zwitterion macromolecules, with the network characteristics depending on the molecular weight of the arms [14].

The conformations of telechelic micelles are evidently determined by the competition between entropic and energetic contributions. A detailed investigation, by theory and simulation, of the mechanisms leading to the formation of collapsed soft spheres is, however, still lacking. In this Letter we perform extensive computer simulations, accompanied by a scaling analysis of the free energies of candidate structures of telechelic micelles with small functionality, $f \leq 5$. We find that at high temperatures the system assumes the usual star burst (*sb*) configuration. On the contrary, at sufficiently low temperatures, the end-monomers attach to each other and the micelles assume an overall closed configuration, akin to the collapsed soft spheres conjectured in the experimental study of Ref. [4]. Due to the peculiar shape of these aggregates, featuring two points of aggregation, one at each end, we term them "water melons" (*wm*). For intermediate temperatures, the macromolecules exhibit several configurations that correspond to a partial assembling of the terminal groups. The number of chains connected at their ends depends on the temperature T, the functionality f and the degree of polymerization N of the chains. In particular, at a given, sufficiently low T, the *wm*-configuration becomes more stable with respect to the *sb*-one with decreasing N and increasing f, as will be demonstrated in what follows. Our theoretical predictions are found to agree well with simulation results.

We employed monomer-resolved molecular dynamics (MD) simulations to examine the conformations of isolated telechelic micelles. The monomers were modeled as soft spheres interacting by means of a truncated and shifted Lennard-Jones potential, $V_{\rm LJ}^{\rm tr}(r)$ (length scale $\sigma_{\rm LJ}$, energy scale ε), the truncation point being at the minimum, $r_{\rm min} = 2^{1/6}\sigma_{\rm LJ}$, rendering the interaction purely repulsive. The *end-monomers*, on the other hand, interact with each other by means of the *full* Lennard-Jones potential, $V_{\rm LJ}(r)$ that has a minimum value $V_{\rm LJ}(r_{\rm min}) = -\varepsilon$. The chain connectivity was modeled by employing the finite extension nonlinear elastic (FENE) potential [16], using the same parameter values as in the simulation of normal star polymers [17, 18]. The monomer mass m, the energy ε and the length $\sigma_{\rm LJ}$ are assigned the value unity, defining thereby the characteristic time $\tau = m\sigma_{\rm LJ}^2/\varepsilon$ and the dimensionless temperature $T^* = k_{\rm B}T/\varepsilon$, where $k_{\rm B}$ is Boltzmann's constant. The equations of motion were integrated using the velocity form of Verlet's algorithm [19], whereas the temperature was fixed by applying a Langevin thermostat [20]. The timestep was $\Delta t = 10^{-3}\tau$, with a total of 2×10^5 timesteps used for equilibration and 10 independent runs of 5×10^7 timesteps each to gather statistics. The characteristic quantities measured were the

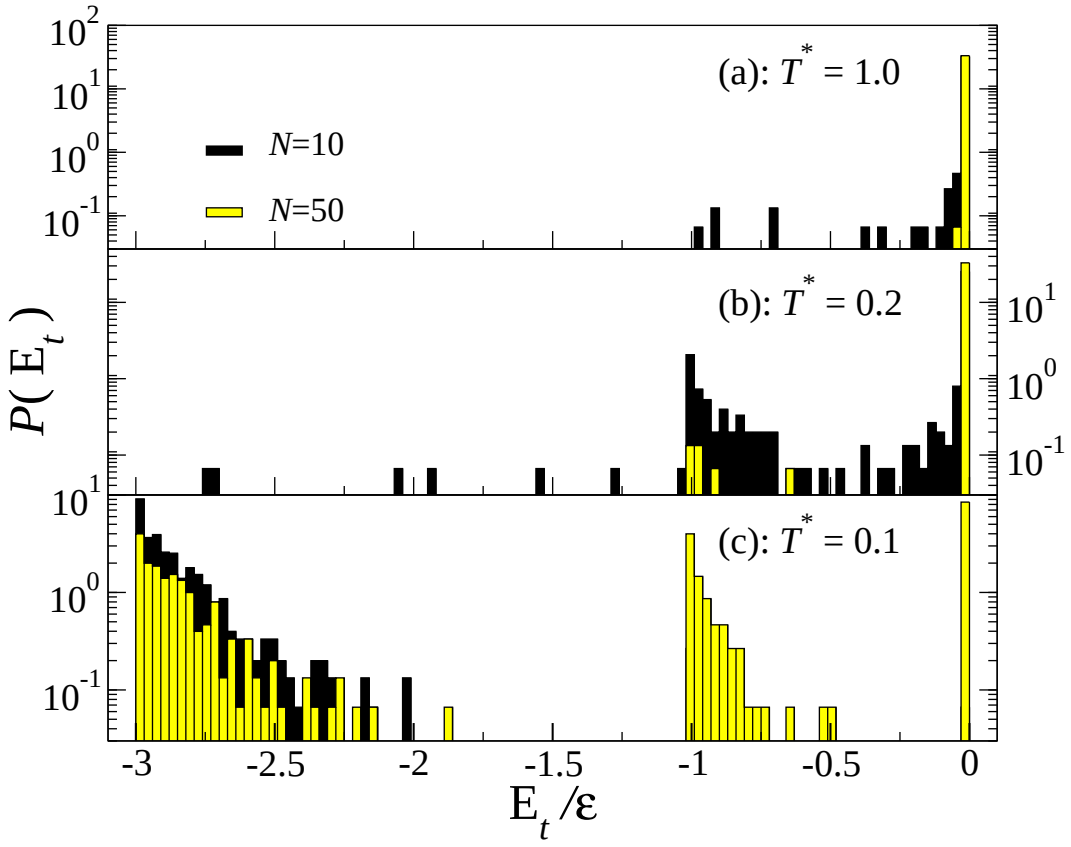

FIG. 1: The probability distribution function $P(E_t)$ obtained from simulations of $f = 3$ telechelic micelles carrying $N = 10, 50$ monomers per arm. Note the logarithmic scale.

radius of gyration R_g of the molecules, the radial distribution function $g_t(r)$ between the terminal monomers and the expectation value E_t of the interaction between the terminal groups, with $E_t = \langle \sum_{i=1}^{f} \sum_{j>i} V_{\rm LJ}(|\mathbf{t}_i - \mathbf{t}_j|) \rangle$, where $\langle \cdots \rangle$ denotes a statistical average and $\mathbf{t}_i$ stands for the position vector of the end-monomer of the i-th chain.

We considered temperatures between $T^* = 0.01$ and $T^* = 1.2$. For $T^* \gtrsim 0.2$, we found that the micelle configuration is similar to that of a star polymer without attractive ends, i.e., the *sb*-configuration. A morphological transition of the micelles takes place upon lowering the temperature. In Fig. 1 we show the probability distribution function $P(E_t)$ for the end-monomer interaction energy E_t for the case $f = 3$, for different T^*- and N-values. Let us focus on $N = 10$. At $T^* = 1.0$, Fig. 1(a), $P(E_t)$ shows almost all the events around $E_t = 0$, meaning that in the vast majority of configurations the end-monomers are far apart, so that the attractions are vanishing. For $T^* = 0.2$, Fig. 1(b), $P(E_t)$ takes a

bimodal form with two peaks, one at $E_t = 0$ and one at $E_t = -\varepsilon$. The latter corresponds to a conformation in which two chains are end-attached, with their terminal monomers at a distance $r_{\min}$, whereas the third chain is still free (intermediate configuration). Note that the molecule does fluctuate between the two conformations, as witnessed both by the bimodal character of the probability distribution and by the non-vanishing values of $P(E_t)$ for $-\varepsilon < E_t < 0$. Upon further lowering of the temperature at $T^* = 0.1$, Fig. 1(c), $P(E_t)$ develops a peak at $E_t = -3\varepsilon$, corresponding to a configuration in which *all three* terminal monomers are confined at a distance $r_{\min}$ from each other. This is the state in which the micelle has aggregation points at both ends, which we termed 'water melon' (*wm*)-conformation. The trend described above persists for $N = 50$. However, in each panel we can notice a higher probability to have association among chains by decreasing N. We further found a considerable sharpening of the peak at $E_t = -3\varepsilon$ for lowered temperatures, since fluctuations around the ground state are getting more suppressed.

Similar results have been found for the cases $f = 2$, 4, and 5. At fixed N, the probability of chain association grows increasing f. The minimum value of E_t for $f = 2$ is $-\varepsilon$ and for $f = 4$ it is -6ε, corresponding to a *wm*-configuration in which *every* end-monomer is confined at a distance $r_{\min}$ from every other one, i.e., an arrangement at the vertices of a regular tetrahedron of edge length $r_{\min}$. Due to geometrical constraints, for $f = 5$ it is not possible to have all five end-monomers at contact with each other; the minimum value for E_t is -9ε in this case, corresponding to the arrangement of the terminal segments on the vertices of *two* regular tetrahedra of edge length $r_{\min}$, which share a common face.

The temperature dependence of the gyration radius R_g for fixed $N = 10$ and different f-values is shown in the main plot of Fig. 2. At high temperatures, R_g has a plateau that corresponds to *sb*-case and scales as $f^{1/5}N^{3/5}$ [21]. As T^* is lowered, we find a rapid decrease of R_g within a narrow temperature range and a saturation to a lower plateau value that corresponds to the size of the *wm*-configuration. The attachment of the terminal monomers leads to a shrinking of the molecule, in agreement with the experimental findings of collapsed soft-sphere conformations [4]. The *wm*-configuration persists to higher T^*-values upon increasing the functionality f, a trend that can be attributed to the increasingly strong attractive-energy contributions to the *wm*-free energy as f grows. In the inset of Fig. 2 we show the terminal-segment radial distribution function for the various f-values at $T^* = 0.1$, where the *wm*-conformation is stable and compare it with the one obtained for $f = 3$

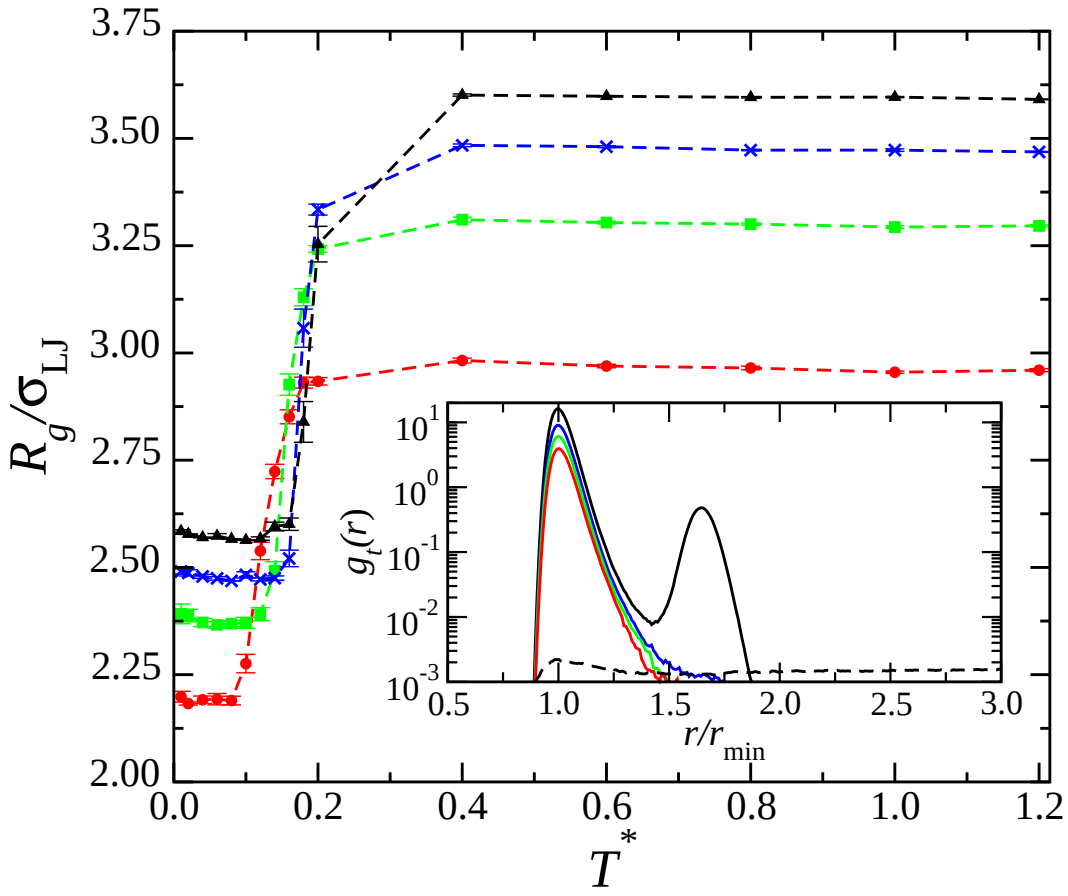

FIG. 2: (Color online) Temperature dependence of the gyration radius R_g obtained by MD of telechelic micelles with $N = 10$. From top to bottom: $f = 5$ (black), $f = 4$ (blue), $f = 3$ (green), and $f = 2$ (red). Inset: the end-monomer radial distribution function $g_t(r)$ obtained from MD at $T^* = 0.1$ (solid curves); the sequence from top to bottom and the color coding are the same as those in the main plot. The dashed line is $g_t(r)$ for $f = 3$ and $T^* = 1.0$ for comparison. For clarity, each curve has been multiplied by a different constant.

at $T^* = 1.0$, where the micelles assume a *sb*-conformation. The aggregation of the end-monomers is clearly witnessed by the high peak at $r = r_{\min}$, which is present at $T^* = 0.1$, as opposed by the flat shape of $g_t(r)$ at $T^* = 1.0$. Whereas for $f = 2$, 3 and 4 a single accumulation peak can be seen, a double peak is present for the case $f = 5$. This feature arises from the arrangement of the five terminal monomers at the vertices of two tetrahedra that share a common face. The most distant vertices of the two are separated by a distance $\sqrt{8/3}r_{\min}$, at which indeed the second peak in $g_t(r)$ shows up.

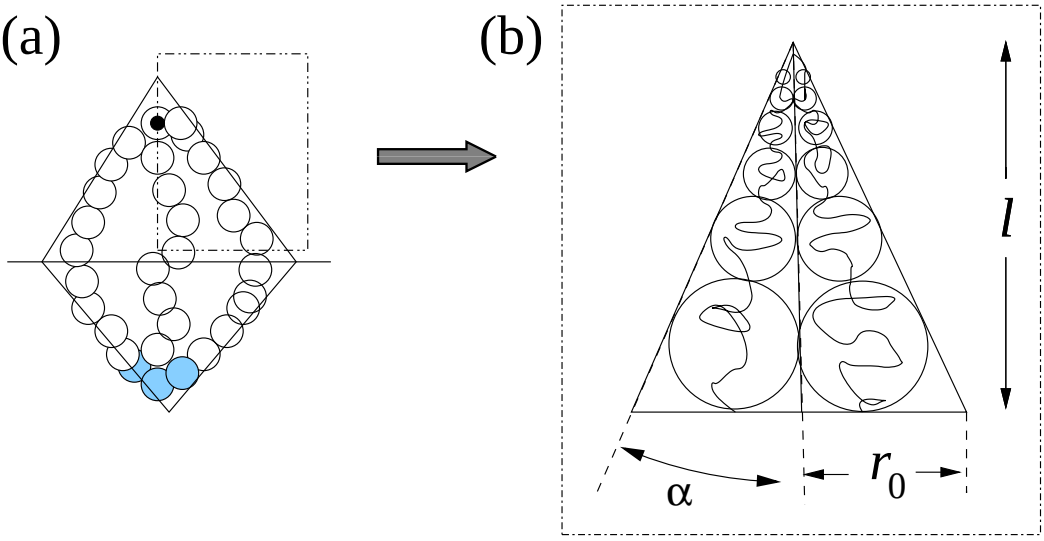

FIG. 3: (a) Schematic representation of a water-melon with $f = 3$ arms, modeled as a double cone of half-chains; (b) the corresponding blob model of two arbitrary, attached arms.

For the theoretical analysis, we consider the *sb*- and *wm*-configurations and put forward a scaling theory, to determine the free energy F of each and find the stable one (lowest F-value). The excluded volume parameter v is set to unity, consistent with the choice $\sigma_{\rm LJ} = 1$ above ($v \cong \sigma_{\rm LJ}^3$). In the case of the *sb*-configuration, the free energy is entirely entropic in nature and can be expressed as a sum of the elastic and excluded-volume contributions. For a single chain, minimization of this sum with respect to the chain radius R_g leads to the scaling laws $R_g \sim N^{3/5}$ and $F \sim k_{\rm B}TN^{1/5}$. For high-functionality star polymers, Flory theory can be improved in order to better take into account the inter-chain correlations by invoking the blob model of Daoud and Cotton [21, 22]. For the small f-values at hand, we envision instead each chain as a blob of radius $\sim R_g$ that occupies a section of space delimited by a solid angle $4\pi/f$. Accordingly, the total free energy of the *sb*-configuration is approximated by $F_{sb} = k_{\rm B}TfN^{1/5}$. The attractive contribution of the terminal monomers is very small, since the latter are far apart in the *sb*-state, and it can thus be ignored.

In the *wm*-configuration, there are two accumulation points: the first is the point in which the chains are chemically linked and the second is at the other end, at which the end-monomers stick together. In order to properly take into account the monomer correlations within the macromolecule [23], we employ a blob model to estimate the excluded-volume contributions to the free energy F_{wm} [10, 24]. A schematic representation of the water melon

and the associated blob model are shown in Fig. 3; the *wm* is thereby modeled as a double cone. With r_0 and l being the radius and height of the cone that contains n_b blobs of a single chain, we obtain

$$\frac{F_{wm}}{k_{\rm B}T} = \frac{3}{2} f \frac{r_0^2 + l^2}{N} + 2 f n_b + E_{\rm attr}. \tag{1}$$

The first term at the right-hand side of Eq. (1) above is the stretching contribution of f chains, each having an extension $\sqrt{r_0^2 + l^2}$. The second is the excluded-volume cost and arises from the total number of $2fn_b$ blobs, each contributing an amount $k_{\rm B}T$ [10, 23, 24]. Finally the third term is the attractive energy contribution arising from the total number of contacts between terminal monomers. Accordingly, $E_{\rm attr} = -f(f-1)/(2T^*)$ for $f = 2$, 3, and 4, whereas $E_{\rm attr} = -9/T^*$ for $f = 5$. The blobs are close-packed within each cone, hence:

$$\frac{l}{\cos(\alpha/2)} = D \sum_{n=0}^{n_b - 1} \left(\frac{1 + \sin(\alpha/2)}{1 - \sin(\alpha/2)} \right)^n, \tag{2}$$

where $\alpha = \arctan(r_0/l)$ is the cone opening angle and D is the diameter of the first, smallest blob, taken equal to the monomer size. The polymerization N is obtained by summing over the monomers of all blobs of a chain, taking into account that a blob of size b contains $N_b \sim b^{5/3}$ monomers. This yields

$$N(r_0, l) = 2D^{5/3} \sum_{n=0}^{n_b - 1} \left(\frac{1 + \sin(\alpha/2)}{1 - \sin(\alpha/2)} \right)^{(5n/3)}. \tag{3}$$

We solved Eqs. (2) and (3) numerically to express n_b and l in terms of r_0 and then we minimized numerically F_{wm} with respect to r_0 using Eq. (1). We found that the cone angle α between two arms increases rapidly with N for small N-values: for $5 \lesssim N \lesssim 20$ it changes from 20 to 40 degrees. This trend reflects the physical difficulty for the chains to form an aggregate for short chains, due to strong steric hindrance at the star center. Once the excluded volume interactions are balanced, the angle increases slowly, by about 5 degrees for $25 \lesssim N \lesssim 400$.

Comparing the minimized free energies F_{wm} with F_{sb}, we obtained the *transition* temperature between *sb* and *wm* as a function of N [26]. In Fig. 4 we show the T vs. N transition lines, separating the *wm*-state (below) from the *sp*-one (above). The 'critical number' N_c increases with decreasing T^* and the transition temperature increases with f. Stated otherwise, for fixed N the theoretical model gives evidence to a stronger stability of the *wm* configuration on increasing f and lowering the temperature. On the other hand, keeping f

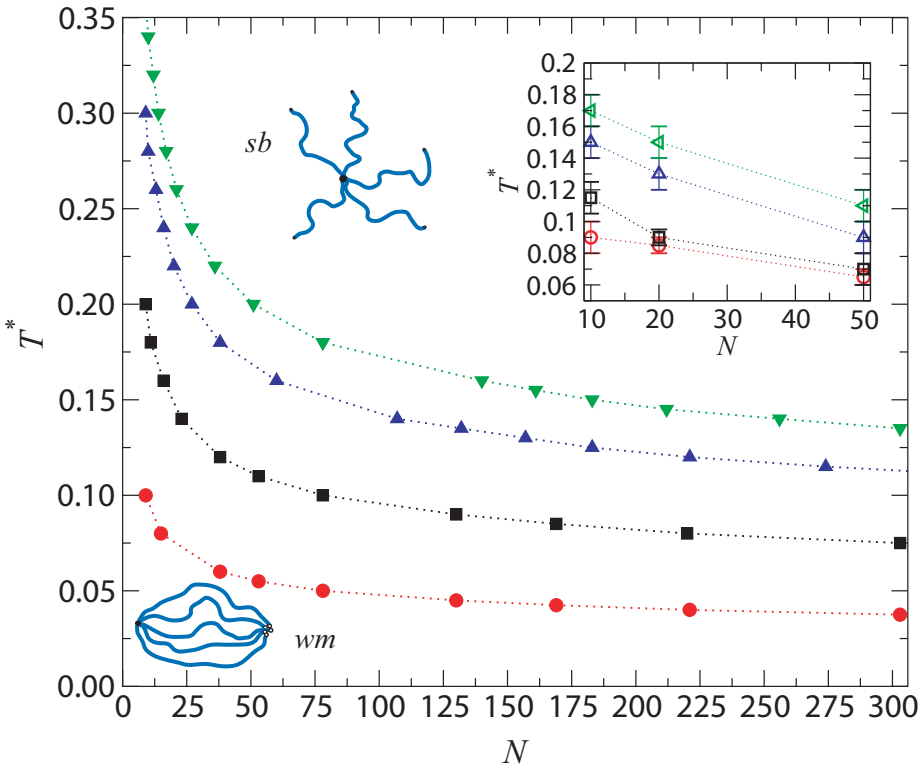

FIG. 4: Temperature versus N diagram corresponding to the *sb*- and *wm*-morphological transitions of telechelic micelles. Main figure: theoretical results. Inset: transition lines in simulations, determined via the T^* dependence of R_g . From bottom to top (full/empty symbols): $f = 2$ (circle), $f = 3$ (square), $f = 4$ (triangle up), $f = 5$ (triangle down).

and T^* fixed, the *sb*-configuration is stable above a certain value of N_c. The dependence of the repulsive contribution in the free energy on the number of monomers is not trivial: increasing N, the number of blobs n_b increases and so does the contribution due to the excluded volume interaction. The entropic contribution is proportional to r_0^2, which increases with N, and to $1/N$. The balance between all these terms in Eq. (1) determines the stable micelle conformation: it is physically more expensive for the molecule to assume a *wm*-configuration the lower f and the higher N is. N_c decreases rapidly with T^* and the *wm*-state becomes unstable at $T^* \gtrsim 0.3$ for all f-values considered. In the inset of Fig. 4 we show the corresponding MD-results: notice the nice agreement with the theoretical prediction trends. The value of transition temperature is overestimated in theory, reflecting the mean-field nature of the latter. There exist also configurations intermediate to the *wm*- and

sb-ones, in which only a partial association of arms takes place, akin to those seen for block-copolymer stars with $f = 12$ in the simulation study of Ref. [8]. Such configurations are also expected to be dominant as f further increases, due to the very high entropic penalty inherent to a complete intramolecular association. These conformations can be analyzed along the lines put forward in this work, since intermediate states can be looked upon as a combination of smaller water melons (work in progress).

We have studied the dependence of the equilibrium conformations of telechelic micelles on the temperature, arm number and functionality of the same. The system presents a stable, water-melon configuration for low temperatures that opens up as T grows. The dynamical properties of such aggregates in solution will have unusual characteristics: at low temperatures and near the overlap concentration, various types of gels can appear, owing their viscosity either to transient network formation or to the existence of entangled loops. An understanding of the changes in the micelle conformations is a relevant starting point, aiming at gaining control over the supramolecular structural and dynamical properties of the system [25], and targeting specific applications.

We thank W. Russel for bringing Refs. [11] and [12] to our attention and D. Vlassopoulos for helpful discussions. C.M. thanks the Düsseldorf Entrepeneurs Foundation for financial support. This work was supported by the DFG within the SFB-TR6 and by the Marie Curie European Network MRTN-CT-2003-504712.

---

[1] M. Muthukumar *et al.*, Science **277**, 1225 (1997).

[2] *Theoretical Challenges in the Dynamics of Complex Fluids*, edited by T. C. B. McLeish, NATO ASI Vol. 339 (Kluwer, London, 1997).

[3] M. Pitsikalis *et al.*, Macromolecules **29**, 179 (1996).

[4] D. Vlassopoulos *et al.*, J. Chem. Phys. **111**, 1760 (1999).

[5] F. Clément *et al.*, Macromolecules **33**, 6148 (2000).

[6] Yu. D. Zaroslov *et al.*, Macromol. Chem. and Phys. **206**, 173 (2005).

[7] F. Ganazzoli *et al.*, Macromol. Theory Simul. **10**, 325 (2001).

[8] R. Connolly *et al.*, J. Chem. Phys. **119**, 8736 (2003).

[9] A. N. Semenov *et al.*, Macromolecules **28**, 1066 (1995).

[10] A. G. Zilman and S. A. Safran, Eur. Phys. J. E **4**, 467 (2001).

[11] X.-X. Meng and W. B. Russel, Macromolecules **36**, 10112 (2003).

[12] S. R. Bhatia and W. B. Russel Macromolecules **33**, 5713 (2000).

[13] U. Batra *et al.*, Macromolecules **30**, 6120 (1997).

[14] D. Vlassopoulos *et al.*, Macromolecules **33**, 9740 (2000).

[15] M. Pitsikalis and N. Hadjichristidis, Macromolecules **28**, 3904 (1995).

[16] M. J. Stevens and K. Kremer, Phys. Rev. Lett. **71**, 2228 (1993).

[17] G. S. Grest *et al.*, Macromolecules **20** 1376 (1987).

[18] G. S. Grest *et al.*, Adv. Chem. Phys. **XCIV**, 67 (1996).

[19] M. P. Allen, D. J. Tildesley *Computer Simulation of liquids* (Oxford University Press, Oxford, 1987).

[20] K. Kremer and G. S. Grest, J. Chem. Phys. **92**, 5057 (1990).

[21] M. Daoud and J. P. Cotton, J. Physique **43**, 531 (1982).

[22] T. A. Witten and P. A. Pincus, Macromolecules **19**, 2509 (1986).

[23] A. Yu. Grosberg and A. R. Khokhlov, *Statistical Physics of Macromolecules* AIP Press, New York, 1994.

[24] P. G. de Gennes, in *Solid State physics, Supplement 14: Liquid Crystals*, edited by H. Ehrenreich, F. Seitz, D. Turnbull and L. Liebert, (Academic, New York, 1978).

[25] G. Arya and A. Z. Panagiotopoulos, Phys. Rev. Lett. **95**, 188301 (2005).

[26] As we are dealing with finite systems, these are not sharp transitions but rather crossover phenomena.